1-1-2019

Modulating GLUT1 Expression in Retinal Pigment Epithelium Decreases Glucose Levels in the Retina: Impact on Photoreceptors and Müller Glial Cells

Aditi Swarup

Ivy S. Samuels

Brent A. Bell
University of Pennsylvania

John Y.S. Han

Jianhai Du

See next page for additional authors

Recommended Citation

Swarup, A., Samuels, I. S., Bell, B. A., Han, J. Y., Du, J., Massenzio, E., Abel, E. D., Boesze-Battaglia, K., Peachey, N. S., & Philp, N. J. (2019). Modulating GLUT1 Expression in Retinal Pigment Epithelium Decreases Glucose Levels in the Retina: Impact on Photoreceptors and Müller Glial Cells. *American Journal of Physiology - Cell Physiology, 316* (1), C121-C133. Retrieved from https://repository.upenn.edu/dental_papers/405

Modulating GLUT1 Expression in Retinal Pigment Epithelium Decreases Glucose Levels in the Retina: Impact on Photoreceptors and Müller Glial Cells

Abstract

The retina is one of the most metabolically active tissues in the body and utilizes glucose to produce energy and intermediates required for daily renewal of photoreceptor cell outer segments. Glucose transporter 1 (GLUT1) facilitates glucose transport across outer blood retinal barrier (BRB) formed by the retinal pigment epithelium (RPE) and the inner BRB formed by the endothelium. We used conditional knockout mice to study the impact of reducing glucose transport across the RPE on photoreceptor and Müller glial cells. Transgenic mice expressing Cre recombinase under control of the Bestrophin1 (Best1) promoter were bred with Glut1 $^{flox/flox}$ mice to generate Tg-Best1-Cre:Glut1 $^{flox/flox}$ mice (RPEΔGlut1). The RPEΔGlut1 mice displayed a mosaic pattern of Cre expression within the RPE that allowed us to analyze mice with ~50% (RPEΔGlut1 $_{m}$) recombination and mice with >70% (RPEΔGlut1 $_{h}$) recombination separately. Deletion of GLUT1 from the RPE did not affect its carrier or barrier functions, indicating that the RPE utilizes other substrates to support its metabolic needs thereby sparing glucose for the outer retina. RPEΔGlut1 $_{m}$ mice had normal retinal morphology, function, and no cell death; however, where GLUT1 was absent from a span of RPE greater than 100 μm, there was shortening of the photoreceptor cell outer segments. RPEΔGlut1 $_{h}$ mice showed outer segment shortening, cell death of photoreceptors, and activation of Müller glial cells. The severe phenotype seen in RPEΔGlut1 $_{h}$ mice indicates that glucose transport via the GLUT1 transporter in the RPE is required to meet the anabolic and catabolic requirements of photoreceptors and maintain Müller glial cells in a quiescent state.

Keywords

BEST1-cre; GLUT1; Müller glial cells; Photoreceptor cells; Retina

Disciplines

Dentistry

Author(s)

Aditi Swarup, Ivy S. Samuels, Brent A. Bell, John Y.S. Han, Jianhai Du, Erik Massenzio, E. Dale Abel, Kathleen Boesze-Battaglia, Neal S. Peachey, and Nancy J. Philp

Am J Physiol Cell Physiol 316: C121–C133, 2019.
First published November 21, 2018; doi:10.1152/ajpcell.00410.2018.

RESEARCH ARTICLE

Modulating GLUT1 expression in retinal pigment epithelium decreases glucose levels in the retina: impact on photoreceptors and Müller glial cells

Aditi Swarup,[1] Ivy S. Samuels,[2,3] Brent A. Bell,[4] John Y. S. Han,[1] Jianhai Du,[5] Erik Massenzio,[1] E. Dale Abel,[6,7] Kathleen Boesze-Battaglia,[8] Neal S. Peachey,[2,3,9]* and Nancy J. Philp[1]*

[1]*Department of Pathology, Anatomy and Cell Biology, Thomas Jefferson University, Philadelphia, Pennsylvania;* [2]*Louis Stokes Cleveland VA Medical Center, Cleveland, Ohio;* [3]*Cole Eye Institute, Cleveland Clinic, Cleveland, Ohio;* [4]*Department of Ophthalmology, University of Pennsylvania, Philadelphia, Pennsylvania;* [5]*Department of Ophthalmology, Department of Biochemistry, West Virginia University Eye Institute, Morgantown, West Virginia;* [6]*Fraternal Order of Eagles Diabetes Research Center, University of Iowa, Iowa City, Iowa;* [7]*Division of Endocrinology and Metabolism, Carver College of Medicine, University of Iowa, Iowa City, Iowa;* [8]*Department of Biochemistry, Penn Dental Medicine, University of Pennsylvania, Philadelphia, Pennsylvania; and* [9]*Department of Ophthalmology, Cleveland Clinic Lerner College of Medicine of Case Western Reserve University, Cleveland, Ohio*

Submitted 18 October 2018; accepted in final form 19 November 2018

Swarup A, Samuels IS, Bell BA, Han JY, Du J, Massenzio E, Abel ED, Boesze-Battaglia K, Peachey NS, Philp NJ. Modulating GLUT1 expression in retinal pigment epithelium decreases glucose levels in the retina: impact on photoreceptors and Müller glial cells. *Am J Physiol Cell Physiol* 316: C121–C133, 2019. First published November 21, 2018; doi:10.1152/ajpcell.00410.2018.—The retina is one of the most metabolically active tissues in the body and utilizes glucose to produce energy and intermediates required for daily renewal of photoreceptor cell outer segments. Glucose transporter 1 (GLUT1) facilitates glucose transport across outer blood retinal barrier (BRB) formed by the retinal pigment epithelium (RPE) and the inner BRB formed by the endothelium. We used conditional knockout mice to study the impact of reducing glucose transport across the RPE on photoreceptor and Müller glial cells. Transgenic mice expressing *Cre recombinase* under control of the Bestrophin1 (*Best1*) promoter were bred with $Glut1^{flox/flox}$ mice to generate $Tg\text{-}Best1\text{-}Cre{:}Glut1^{flox/flox}$ mice (*RPEΔGlut1*). The *RPEΔGlut1* mice displayed a mosaic pattern of *Cre* expression within the RPE that allowed us to analyze mice with ~50% ($RPE\Delta Glut1_m$) recombination and mice with >70% ($RPE\Delta Glut1_h$) recombination separately. Deletion of GLUT1 from the RPE did not affect its carrier or barrier functions, indicating that the RPE utilizes other substrates to support its metabolic needs thereby sparing glucose for the outer retina. $RPE\Delta Glut1_m$ mice had normal retinal morphology, function, and no cell death; however, where GLUT1 was absent from a span of RPE greater than 100 μm, there was shortening of the photoreceptor cell outer segments. $RPE\Delta Glut1_h$ mice showed outer segment shortening, cell death of photoreceptors, and activation of Müller glial cells. The severe phenotype seen in $RPE\Delta Glut1_h$ mice indicates that glucose transport via the GLUT1 transporter in the RPE is required to meet the anabolic and catabolic requirements of photoreceptors and maintain Müller glial cells in a quiescent state.

BEST1-cre; GLUT1; Müller glial cells; photoreceptor cells; retina

INTRODUCTION

The neural retina is one of the most metabolically active tissues in the body. Otto Warburg determined over a hundred years ago that the retina is highly glycolytic and converts nearly 80% of glucose into lactate through aerobic glycolysis (6, 53). The retina is supported by two blood supplies: the choroidal blood supply and the inner retinal vasculature (8). The choroidal vasculature is very dense and is composed of fenestrated capillaries that underlie the retinal pigment epithelium (RPE), which forms the outer blood retinal barrier (BRB). Glucose transporter 1 (GLUT1) is expressed at high levels in the apical and basolateral membranes of the RPE and in the inner BRB where it is located in the luminal and abluminal membranes of the endothelial cells (19, 47). Thus, GLUT1 is well positioned to facilitate the transepithelial transport of glucose into the outer and inner retina (20).

The choroidal circulation has been shown to deliver nutrients and oxygen to the outer retina and remove metabolic waste via the RPE (13, 27). Previous studies have examined the effects of disrupting the choroidal vessels on photoreceptor health highlighting the importance of the choroidal vessels in supplying nutrients and oxygen to the outer retina. In these mice, flow of both oxygen and nutrients was disrupted leading to metabolic reprograming of the RPE and photoreceptor cell death (21, 22).

In the current study, we knocked out a single metabolic transporter from the RPE, GLUT1, to determine the importance of glucose transport across the outer BRB in supporting outer retinal structure, function, and viability. We found that genetic deletion of GLUT1 in the RPE did not affect its barrier properties or state of differentiation, supporting studies that show that the RPE is oxidative and utilizes lactate, amino acids, and fatty acids as metabolic substrates (1, 2, 16). However, decreased transport of glucose into the outer retina of *RPEΔGlut1* mice decreased retinal glucose levels, affected outer segment renewal and photoreceptor cell survival, and resulted in activation of Müller glial cells. There was a greater impact on rod photoreceptor cells than on cone photoreceptor

* N. S. Peachey and N. J. Philp are co-senior authors.
Address for reprint requests and other correspondence: N. J. Philp, Department of Pathology Anatomy and Cell Biology, Thomas Jefferson University, 1020 Locust St., Philadelphia, PA 19107 (e-mail: nancy.philp@jefferson.edu).

cells, suggesting that rods are more dependent on glycolytic metabolism than cones.

MATERIALS AND METHODS

Animals. Mice carrying the homozygous floxed *Slc2a1* allele (55) were crossed to a transgenic line that expressed *Cre recombinase* under control of the promoter for Bestrophin1 (*BEST1*; Jax stock no. 017557) (14). We used a two-generation cross to generate mice that were *Slc2a1*$^{loxP/loxP}$ homozygous and *Cre* transgenic, as well as control littermates. All animal procedures were conducted with the approval of the Thomas Jefferson University or Louis Stokes Cleveland VA Medical Center Institutional Animal Care and Use Committees and conformed to the Association for Research in Vision and Ophthalmology (ARVO) statement for use of animals in ophthalmic and vision research.

Spectral domain-optical coherence tomography. Mice were anesthetized with a mixture of ketamine (100 mg/kg) and xylazine (10 mg/kg), after which the pupils were dilated with eye drops (1% phenylephrine HCl ophthalmic solution, Akorn, Lake Forest, IL). A Bioptigen (Durham, NC) SD-OCT system was used to image the eyes at 840 nm. Retinas were imaged at 1.4 mm radial measurement of 1,000 A-scans by two B-scans per image and averaged over 15 images. Bioptigen InVivoVue software was used to average the images.

Immunofluorescence. Mice were anesthetized with ketamine (100 mg/kg) and xylazine (10 mg/kg) and euthanized by cervical dislocation following enucleation of the eyes. Eyes were fixed in cold (−80°C) methanol:acetic acid (97:3) as previously described (45). For immunofluorescence, the fixed eyes were processed for embedding in optimal cutting temperature (OCT) compound and blocks were stored at −80°C. Sections (10 μm) were cut and placed on positively charged glass slides. Sections were blocked in 5% BSA in phosphate-buffered saline (PBS) with 0.1% Tween (PBST) for 1 h then incubated in primary antibody (Table 1) diluted in 1% BSA in PBST overnight at 4°C. Sections were incubated at room temperature with secondary antibodies (Table 1) and with DAPI, and then imaged on an LSM 780 NLO laser scanning microscope (Carl Zeiss, Oberkochen, Germany) using ApoPlan ×63/1.4 objective and EC NeoPlan ×10/0.3 objective. For hematoxylin and eosin (H&E)-stained sections, methanol:acetic acid fixed eyes were embedded in paraffin and 10-μm sections were cut as described previously (46). Paraffin sections were deparaffinized using xylene and rehydrated in a graded series of ethanol then water and used for immunofluorescence labeling as described above.

Western blotting. RPE was isolated from control and *RPEΔGlut1* as previously described (52) and homogenized in 50 μl radioimmunoprecipitation assay (RIPA, Thermo Scientific, Rockford, IL) with protease inhibitors and extracted on ice for 30 min. Samples were centrifuged for 30 min at 15,000 *g* and the supernatants were removed for protein determination and Western blot analysis. Protein was measured using BCA Protein Assay kit (catalog no. 23225, Thermo Fisher Scientific, Rockford, IL). A total of 5 μg of RPE protein was loaded on 4–12% NuPage Bis-Tris Protein gels (Invitrogen, NP0321BOX) and electrophoretically transferred onto Immobilon-P membrane (Millipore, Bedford, MA). Membranes were incubated for 1 h at room temperature in blocking buffer [5% powdered milk in Tris-buffered saline with 0.1% Tween 20 (TBST)] then incubated overnight with antibodies (Table 1). Membranes were washed three times with TBST and incubated for 1 h with secondary antibody. Blots were developed using chemiluminescence (Supersignal West Dura, Thermo Fisher Scientific, Waltham, MA) on FluorChem M ProteinSimple (San Jose, CA) detection system. Densitometry analysis was performed using FluorChem M ProteinSimple software and normalized to β-catenin.

Quantitative PCR. Isolated RPE and retina were homogenized in 1 ml TRIzol (catalog no. 15596026, Thermo Fisher Scientific). RNA was extracted according to manufacturer specifications. RNA (1 μg) was reverse transcribed to 20 μl cDNA using EcoDry Premix [oligo(dT) catalog no. 639543 Takara Bio USA, Mountain View, CA]. qPCR was performed using 0.5 μl of cDNA and PowerUp SYBR Green Master Mix (Thermofisher, cat. no. A25742) on a QuantStudio 5 Real-Time PCR System (Thermofisher, cat. no. A28139). The PCR reaction was heated to 50°C for 2 min and held at 95°C for 10 min to activate the polymerase. Amplification was performed for 40 cycles of 15 s, denaturing at 95°C, and 1 min of annealing at 60°C. Cycle threshold (Ct) values were normalized to RPLP0 (Table 2).

Flatmounts of RPE. Mice were anesthetized with ketamine (100 mg/kg) and xylazine (10 mg/kg) and euthanized by cervical dislocation following enucleation of the eyes. Eyes were fixed in 4% paraformaldehyde (PFA) for 8–10 min, in a 96-well plate, after which they were transferred to 1× Dulbecco's PBS (DPBS) (Corning, 21-030-CV). Extraocular muscles and connective tissues attached to the eye were cut away using fine forceps and scissors. The anterior segment of the eye was removed using a razor blade and the retina was removed using fine forceps. The posterior eyecup was fixed in 4% PFA for an additional 8 min and subsequently washed with 1× DPBS. The fixed eyecup was permeabilized in 0.3% Triton X-100 in 1×

Table 1. *Antibodies for immunoblotting and immunofluorescence microscopy*

Antibody	Dilution	Catalog no.	Company
Cone arrestin	1:1,000 (IF)	AB15282	Millipore
Red/green opsin	1:200 (IF)	AB5405	Millipore
Blue opsin	1:200 (IF)	AB5407	Millipore
GFAP	1:1,000 (IF)	SAB4300647	Sigma
GLUT1	1:50 (IF)	MA5-11315	ThermoFisher Scientific
GLUT1	1:250 (IF)1:1,000 (IB)	GT11-A	Alpha Diagnostics
MCT1	1:500 (IF)1:2,000 (IB)	NA	Philp Laboratory
MCT3	1:5,000 (IF,IB)	NA	Philp Laboratory
Rhodopsin	1:100 (IF)	Ab5417	Abcam
P-Cadherin	1:500 (IB)	AF761	R&D Systems
β-Catenin	1:5,000 (IB)	C2206	Sigma Aldrich
Cre	1:100 (IF)	MAB-3120	Millipore
Alexa Fluor 546 donkey anti-rabbit	1:500 (IF)	A10040	ThermoFisher Scientific
Alexa Fluor 555 goat anti mouse	1:500 (IF)	A21422	ThermoFisher Scientific
Alexa Fluor 488 donkey anti-rabbit	1:500 (IF)	A21206	ThermoFisher Scientific
Alexa Fluor 555 donkey anti-mouse	1:500 (IF)	A21202	ThermoFisher Scientific
Bovine anti-goat IgG-HRP	1:2,000 (IB)	Sc-2350	Santa Cruz

HRP, horseradish peroxidase; IB, immunoblotting; IF, immunofluorescence.

Table 2. *List of primers for quantitative PCR*

Primer	Forward	Reverse
Glut1	5′-GGCCTGACTACTGGCTTTGT-3′	5-TGCATTGCCCATGATGGAGT-3′
Glut3	5′-GGTGGAGCGGTGAAGATCAG-3′	5′-GAGATGGGGTCACCTTCGTT-3′
Sglt1	5′-GGATCAGGTCATTGTGCAGC-3′	5′-TGGTGTGCCGCAGTATTTCT-3′
Sglt2	5′-CGGCACTCTTCTGTCGGGTA-3′	5′-GGCGATGGAGATGCTTCTGA-3′
Glut12	5′-GGAGCTAGCAAAGGCGAA-3′	5′-GACTGTCCCCTTCCACACAG-3′
GFAP	5′-GCGAAGAAAACCGCATCACC-3′	5′-TTCTTTGGTGCTTTTGCCCC-3′
Mct1	5′-TGTTAGTCGGAGCCTTCATT-3′	5′ CACTGGTCGTTGCACTGAATA-3′
Mct3	5′-AAGGCTGTGAGCGTCTTCT-3′	5′-GAAGCCAGAATCATGCCTGCT-3′
PCad	5′-GCAGAAGTCAGCGAGAAAGGA-3′	5′-GGAGGATGAAACCACCCTTCCA-3′
Slc38a3	5′-CGTCTCAGCTTTCCGAGAGT-3′	5′-GTCTTCCCCTCGAAATCGGT-3′
Slc1a7	5′-CACAGACCATGGCTGCAAGG-3′	5′-TAACTAATCTCCTGTGGTGAGAGG-3′
Slc7a8	5′-AAACAACACCGCGAAGAACC-3′	5′-GAGCCAATGATGTTCCCTACAA-3′
RPLP0	5′-AGATTCGGGATATGCTGTTGGC-3′	5′-TCGGGTCCTAGACCAGTGTTC-3′

DPBS for 15 min and blocked with 5% BSA 0.1% Triton X-100 for 1 h. The eyecups were incubated in primary antibody overnight in 1% BSA 0.1% Triton X-100 and washed in 1× DPBS (Table 1). Then eyecups were incubated at room temperature with secondary antibody and DAPI in 1% BSA 0.1% Triton X-100 for 1 h. After a final wash in 1× DPBS, eyecups were placed on glass slides, flattened using 4–8 radial cuts, and coverslipped using Gelvatol as a mounting medium. Flatmounts were imaged using a Nikon (Melville, NY) Eclipse E800 fluorescent microscope using the Plan Fluor ×10/0.30 or ×40/0.75 objectives.

TUNEL. Frozen sections prepared from methanol:acetic acid fixed eyes were post-fixed with 4% PFA for 5 min then treated with proteinase K for 15 min. Apoptotic cells were detected by TUNEL assay kit (Millipore, S7110) as per manufacturer's specification.

Cone counts and measurement of outer segment length. Cones were probed with cone arrestin antibody on methanol:acetic acid fixed sections. Cones were counted in 1,500 μm length of retina from both sides of the optic nerve on the horizontal meridian in retinal areas expressing or devoid of GLUT1. Cone outer segment length was determined by colabeling sections with a mixture of red/green and blue opsin and GLUT1 antibodies. Outer segment length was measured using the measurement tool in Photoshop.

Electroretinograms. After overnight dark adaptation, mice were anesthetized (65 mg/kg pentobarbital sodium), the cornea was anesthetized (1% proparacaine HCl), and the pupils were dilated (1% tropicamide, 2.5% phenylephrine HCl, and 1% cyclopentolate). Mice were placed on a temperature-regulated heating pad throughout the recording session. Responses of the outer retina were recorded on an Espion E3 ColorDome Full field Ganzfeld (Diagnosys, Lowell, MA) with an Ag/AgCl electrode referenced to an Ag/AgCl pellet electrode placed in the mouth of the mouse in response to strobe-flash stimuli presented in the dark. Ten steps of increasing flash luminance [−3.6 to 2.1 log candela (cd)·s/m^2] were presented in order of increasing flash strength, and the number of successive trials averaged together decreased from 20 for low-level flashes to 2 for the highest flash stimuli. The duration of the interstimulus interval increased from 4 s for low luminance flashes to 90 s for the highest stimuli. Immediately following the dark-adapted strobe-flash stimuli, the c-wave was recorded in response to a 5 cd/m^2 stimulus presented for 7 min. Immediately after the dark-adapted recording, a steady 20 cd/m^2 adapting field was presented in the ganzfeld bowl. After an additional 4 min of light adaptation, cone electroretinograms (ERGs) were recorded to strobe flash stimuli (−1 to 2 log cd s/m^2) superimposed on the adapting field.

The amplitude of the a-wave was measured 8.32 ms after the flash onset from the pre-stimulus baseline. The dark-adapted b-wave amplitude was measured from the a-wave amplitude at 8.32 ms to the peak of the strobe flash response. The amplitude of the light-adapted ERG was measured from the amplitude of the light-adapted waveform at 8.32 ms to the peak of the response. The amplitude of the c-wave was measured from the prestimulus baseline to the peak of the response.

[^{13}C]glucose labeling and liquid chromatography–mass spectrometry. Mice were injected intraperitoneally with 500 mg/kg [^{13}C]-D-glucose (U-$^{13}C_6$, 99%) (CAS no. 110187-42-3; Cambridge Isotope, Andover, MA). After 45 min, injected mice were anesthetized with ketamine (100 mg/kg) and xylazine (10 mg/kg) and euthanized by cervical dislocation and their retinas were isolated and flash frozen in liquid nitrogen. Metabolites were extracted in 80% methanol and analyzed with a Shimadzu LC Nexera X2 UHPLC coupled with a QTRAP 5500 MS (AB Sciex) as described previously (9, 58). An ACQUITY UPLC BEH Amide analytic column (2.1 × 50 mm, 1.7 μm, Waters) was used for chromatographic separation. The source and collision gas was N_2. The ion source conditions in positive and negative mode were as follows: curtain gas (CUR) = 25 psi; collision gas (CAD) = high; ion spray voltage (IS) = 3,800/−3,800 V; temperature (TEM) = 500°C; ion source gas 1 (GS1) = 50 psi; and ion source gas 2 (GS2) = 40 psi. Each metabolite was tuned with standards for optimal transitions. The extracted multiple reaction monitoring (MRM) peaks were integrated using MultiQuant software (version 3.0.2; AB Sciex).

Classification of mice into RPEΔGlut1$_m$ and RPEΔGlut1$_h$. Prior to euthanasia, mice were imaged using SD-OCT to predict the extent of GLUT1 deletion based on outer nuclear layer (ONL) thickness and ONL "waviness" and ERGs were conducted on some of these animals. After euthanasia, one eye from every animal was used for flatmount preparation, probed with Cre and GLUT1 antibodies, and stained with DAPI. The immunolabeled flatmounts were used to determine the fraction of RPE cells in which GLUT1 was deleted. Cre distribution was quantified by counting the number of Cre-positive nuclei and normalizing with DAPI positive nuclei to determine the total percentage of Cre-positive cells. This analysis was done on three different locations per flatmount and averaged. Mice were classified into two categories based on expression of Cre-*RPEΔGlut1$_m$* when expression of Cre was medium, between 30% and 50%, and *RPEΔGlut1$_h$* when expression of Cre was high, 70% or more. The other eye from the same animal was either used for protein, RNA, biochemical analysis or sectioned for immunolabeling.

Statistics. Unpaired two-tailed Student's *t*-tests were performed to determine *P* values. Ordinary one-way ANOVA was performed when comparing more than two variables, and *P* values were corrected using Bonferroni's correction. $P \leq 0.05$ was considered significant. Data in the figures represent means ± SE from animals with $n \geq 3$ (as indicated in figure legends). All data analysis was done in GraphPad Prism or Microsoft Excel.

RESULTS

RPEΔGlut1 mice have a mosaic pattern of cre expression. In control mouse retinas, GLUT1 was detected in the basolateral and apical membranes of the RPE (Fig. 1*A*) where it is poised to facilitate transepithelial transport of glucose from the choroidal vessels to the outer retina. To study the importance of glucose in supporting the metabolism of the RPE and outer retina, we crossed *BEST1-cre* mice with *Slc2a1*$^{flox/flox}$ mice. The resulting transgenic mice (*RPEΔGlut1)* had a specific deletion of GLUT1 from the RPE (Fig. 1, *B* and *C*). This deletion was, however, patchy with adjoining areas devoid of or retaining GLUT1. This pattern of deletion reflects the well documented patchy expression of *Cre recombinase* in *BEST1-cre* mice (14). In addition to the patchy expression, the overall level of *Cre recombinase* varied across mice, even within litters. To account for this variability, each *RPEΔGlut1* mouse was individually characterized for its transgene distribution pattern by preparing RPE flatmounts from one eye and coimmunolabeling with Cre antibody (Fig. 1, *D–F*) and GLUT1 antibody (Fig. 1, *D′–F′*). We found a mosaic pattern of *Cre* expression in the *RPEΔGlut1* mice and classified them as described in MATERIALS AND METHODS. We also noted that *Cre recombinase* levels were similar between eyes of a given animal.

To determine whether we could use SD-OCT imaging of *RPEΔGlut1* mice to predict the level of *BEST1-Cre* expression, we imaged *RPEΔGlut1* mice between 1.5 and 2 mo of age and

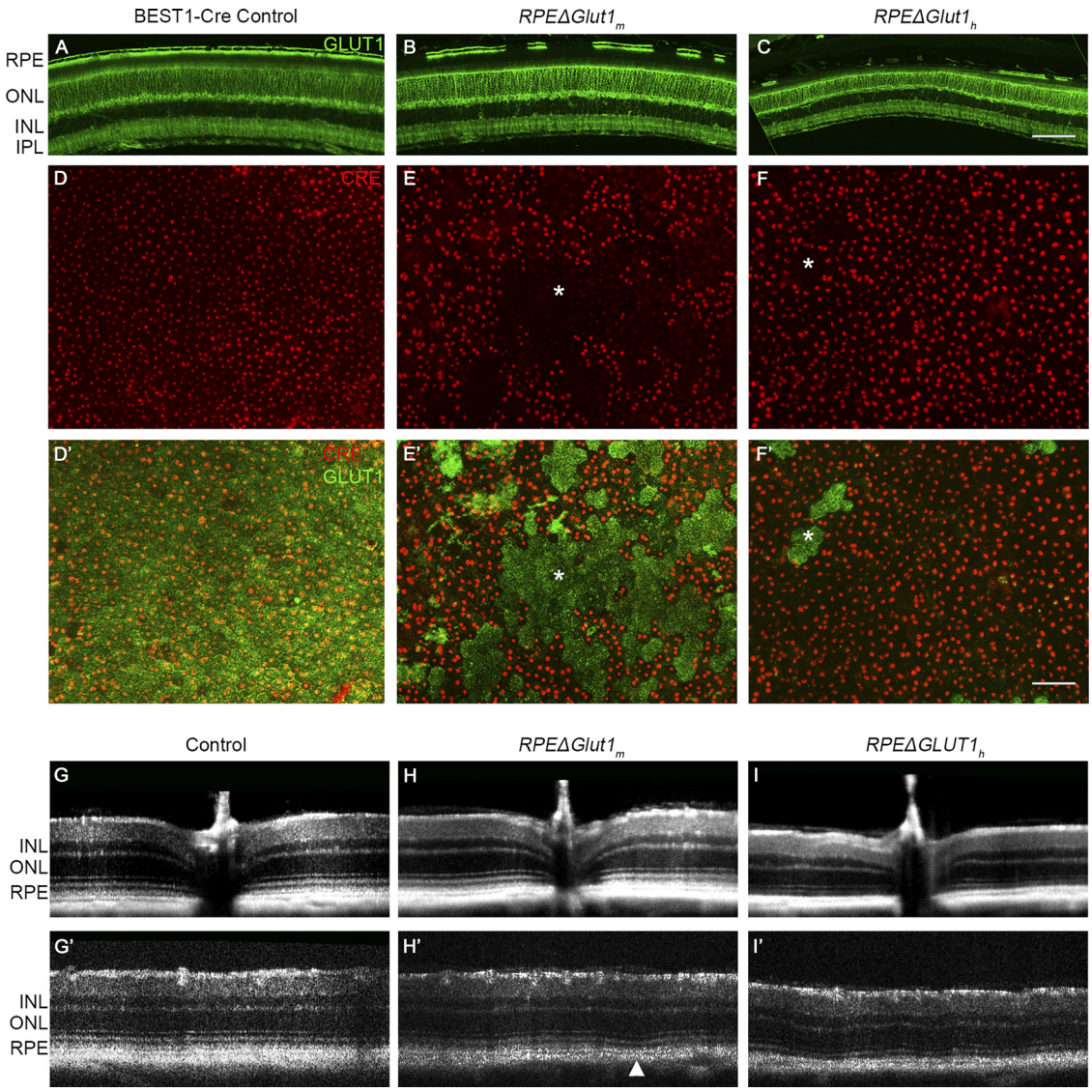

Fig. 1. *RPEΔGlut1* mice show a variable pattern of *Glut1* expression. *A*: methanol:acetic acid-fixed frozen sections from *BEST1-Cre* control mice at age 2 mo show GLUT1 expression in the apical and basal membranes of the RPE. *B*: *RPEΔGlut1*$_m$ mice exhibit intermittent labeling of GLUT1 in the RPE. *C*: *RPEΔGlut1*$_h$ mice have >70% GLUT1 deleted from the RPE. Shown here at age 10 mo. Scale bar, 100 μm. RPE flatmounts immunostained with Cre antibody show a patchy distribution of *Cre*-positive cells. *D–F*: mice were classified into *BEST1-Cre* control (*D*), *RPEΔGlut1*$_m$ (*E*), and *RPEΔGlut1*$_h$ (*F*) based on percentage of *Cre* expression. Coimmunolabeling of RPE flatmounts with GLUT1 and Cre antibodies showed a variable amount of GLUT1 deletion corresponding to the *cre* expression patterns (*D′*, *E′*, *F′*). White asterisks indicate representative regions where *Cre* is not expressed and correspond to where GLUT1 is retained. Scale bar, 100 μm. *G–I*: SD-OCT showing B-scans of retinas from 2-mo-old control (*G*, *G′*), *RPEΔGlut1*$_m$ (*H*, *H′*), and *RPEΔGlut1*$_h$ (*I*, *I′*) mice through the optic nerve and periphery, respectively. INL, inner nuclear layer; IPL, inner plexiform layer; ONL, outer nuclear layer; RPE, retinal pigment epithelium.

then determined *Cre recombinase* levels. We found the ONL thickness of *RPEΔGlut1$_m$* mice ($n = 15$) was indistinguishable from control mice (Fig. 1, *G* and *H*), while SD-OCT B-scans of *RPEΔGlut1$_h$* mice ($n = 20$) showed thinning of the ONL (Fig. 1*I*). *RPEΔGlut1* mice displayed an undulating pattern or "waviness" in the outer retina which was more pronounced in the periphery of the retinal scans. Peripheral B-scans of *RPEΔGlut1$_m$* showed intermittent waviness due to shortening of outer segments (white arrowhead); however, there was no change in ONL thickness in these mice (Fig. 1*H*). *RPEΔGlut1$_h$* mice displayed waviness throughout the retina due to outer segment shortening along with ONL thinning (Fig. 1*I′*). SD-OCT thus provided a robust means to distinguish *RPEΔGlut1$_m$* and *RPEΔGlut1$_h$* mice, based on the observation of waviness and ONL thinning at 2 mo.

Deletion of GLUT1 does not affect differentiation, polarity of monocarboxylate transporter 1/3, or function of RPE. The RPE is highly polarized with differential expression of multiple transporters and ion channels (3, 24). Differentially polarized proteins include two lactate transporters, monocarboxylate transporter 1 (MCT1) that is localized to the apical membrane and monocarboxylate transporter 3 (MCT3) that is localized to the basolateral membrane (30). To determine whether loss of *Glut1* expression led to changes in the properties or differentiation of the RPE, we first compared mRNA expression levels of *Slc16a1* (encoding Mct1) and *Slc16a8* (encoding Mct3) in control and *RPEΔGlut1$_h$* mice (Fig. 2*A*). We also evaluated mRNA levels of *Cdh3* (encoding P-cadherin) a marker of RPE differentiation (56). Despite reduced levels of *Glut1*, no significant difference in expression levels of *Slc16a1, Slc16a8*, or *Cdh3* was observed in *RPEΔGlut1$_h$* mice (Fig. 2*A*). We then compared protein levels of MCT1, MCT3, and P-cadherin using Western blotting, with β-catenin as the loading control (Fig. 2*B*). There was no difference in MCT3 and P-cadherin levels between 3-mo-old control and *RPEΔGlut1$_h$* mice and the decrease in MCT1 levels was not significant (Fig. 2*B*).

Since we did not observe a significant change in mRNA or protein levels of MCT1 and MCT3 in the RPE, we wanted to examine if GLUT1 deletion affected the polarized distribution of these lactate transporters. For this analysis, the patchy distribution of *Cre recombinase* provided an opportunity to compare adjacent regions in the same retina in which GLUT1 was present or absent. In both *RPEΔGlut1$_m$* and *RPEΔGlut1$_h$* mice, MCT1 remained correctly polarized to the RPE apical membrane (see white arrows in Fig. 2, *C*, *C′* and *D*, *D′*) and MCT3 remained correctly polarized to the basolateral membrane (see white arrowheads in Fig. 2, *E*, *E′* and *F*, *F′*) in neighboring areas of RPE that retained or were devoid of GLUT1. We also probed RPE flat mounts with ZO-1 which is localized in cell-cell junctions and can be used to assess changes in size and shape of the cells (11). We noted that the RPE cells of *RPEΔGlut1$_h$* mice retained the classic hexagonal packing and were similar in shape and size to those of control eyes (Fig. 2, *G* and *H*).

These immunohistochemical results indicate that the RPE remains polarized and differentiated in *RPEΔGlut1$_m$* mice. To evaluate the functional status of the RPE in these animals, we examined the ERG c-wave, which reflects a large positive potential generated by hyperpolarization of the apical RPE membrane that is offset somewhat by a negative polarity signal that is generated by the Müller cells (43). The c-wave is an indicator of the integrity of the RPE and is reduced in mouse models of RPE dysfunction (7, 39). In the current studies we measured the c-wave of *RPEΔGlut1$_m$* mice at 4 to 6 mo of age where the scotopic a- and b-waves were indistinguishable from control even though approximately half of the RPE cells are lacking GLUT1 (Fig. 2, *I–K*). Importantly, the amplitude of the c-wave in *RPEΔGlut1$_m$* mice was equivalent to controls. This demonstrates that loss of GLUT1 in the RPE does not affect its barrier properties or polarity. The c-waves of the higher *Cre*-expressing *RPEΔGlut1$_h$* mice were not measured as they would be expected to be abnormal, based on the observed thinning of the ONL, cell death and outer segment shortening. These anatomical changes will directly impact the ERG a- and b-waves, as well as the ERG c-wave since it is generated secondary to photoreceptor activity (41).

GLUT1 is the primary glucose transporter in the RPE and facilitates transport of glucose into the outer retina. We next examined whether there was a compensatory increase in the transcription of other glucose transporters in the RPE of *RPEΔGlut1 mice*. Analysis of the GEO data set GSE10246 (23) demonstrated that *Slc2a1* was the most abundant glucose transporter expressed in the RPE. *Slc2a12*, encoding GLUT12, was also expressed in the control RPE, albeit at much lower levels than *Slc2a1*. When we examined the levels of *Slc2a12* in RPE isolated from 3-mo-old control and *RPEΔGlut1$_h$* mice, we noted no compensatory upregulation of *Slc2a12* in the absence of GLUT1 (Fig. 3*A*). Additionally, no increase in transcript levels of other glucose transporters *Slc2a3*, *Slc5a1*, and *Slc5a2* was detected.

Since there was no compensation for loss of GLUT1 by other glucose transporters, we would expect to find lower levels of glucose in the retina. To test this hypothesis, we performed mass spectrometry analysis on retinas from *Glut1$^{flox/flox}$* control, *RPEΔGlut1$_m$* and *RPEΔGlut1$_h$* mice. The LC/MS analysis showed that the steady-state levels of glucose in the retinas from *RPEΔGlut1$_h$* mice were 32.3 ± 7.8% of control (Fig. 3*B*) and lactate, the end-product of glycolysis, was 46.5 ± 10.6% of control (Fig. 3*C*). There was no significant difference in the glucose or lactate levels between controls and *RPEΔGlut1$_m$* mice. To determine whether differences in steady-state levels of glucose resulted from decreased transport of glucose into the retina, we injected [^{13}C]glucose intraperitoneally and isolated the retinas after 45 min and measured [^{13}C]glucose and lactate using LC/MS. Transport of [^{13}C]glucose into retinas of *RPEΔGlut1$_h$* was 13.4 ± 7.2% of controls (Fig. 3*D*) and [^{13}C]lactate was decreased to 26.9 ± 20.5% of control (Fig. 3*E*). ATP levels did not differ in *RPEΔGlut1$_m$* or *RPEΔGlut1$_h$* mice compared with controls (data not shown).

Longitudinal changes in ONL thickness in RPEΔGlut1$_h$ mice. SD-OCT was used to monitor longitudinal changes in the retinas of *RPEΔGlut1* mice. We imaged *RPEΔGlut1* mice and noted a waviness in the outer retina at 2 mo, which appeared to become more prominent with age. The waviness in the outer retinal layers was caused by a shortening of the photoreceptor cell outer segments and the thinning of the ONL (Fig. 4, *B* and *C*). Between 4 and 6 mo of age, there appeared to be no further reduction in outer segment length or ONL thickness (Fig. 4*D*). The waviness observed by SD-OCT was also evident in H&E stained paraffin sections of eyes from *RPEΔGlut1$_h$* mice (Fig. 4*F*) and corresponded with regions of the retina where the ONL was thinner. No waviness was seen in the sections of

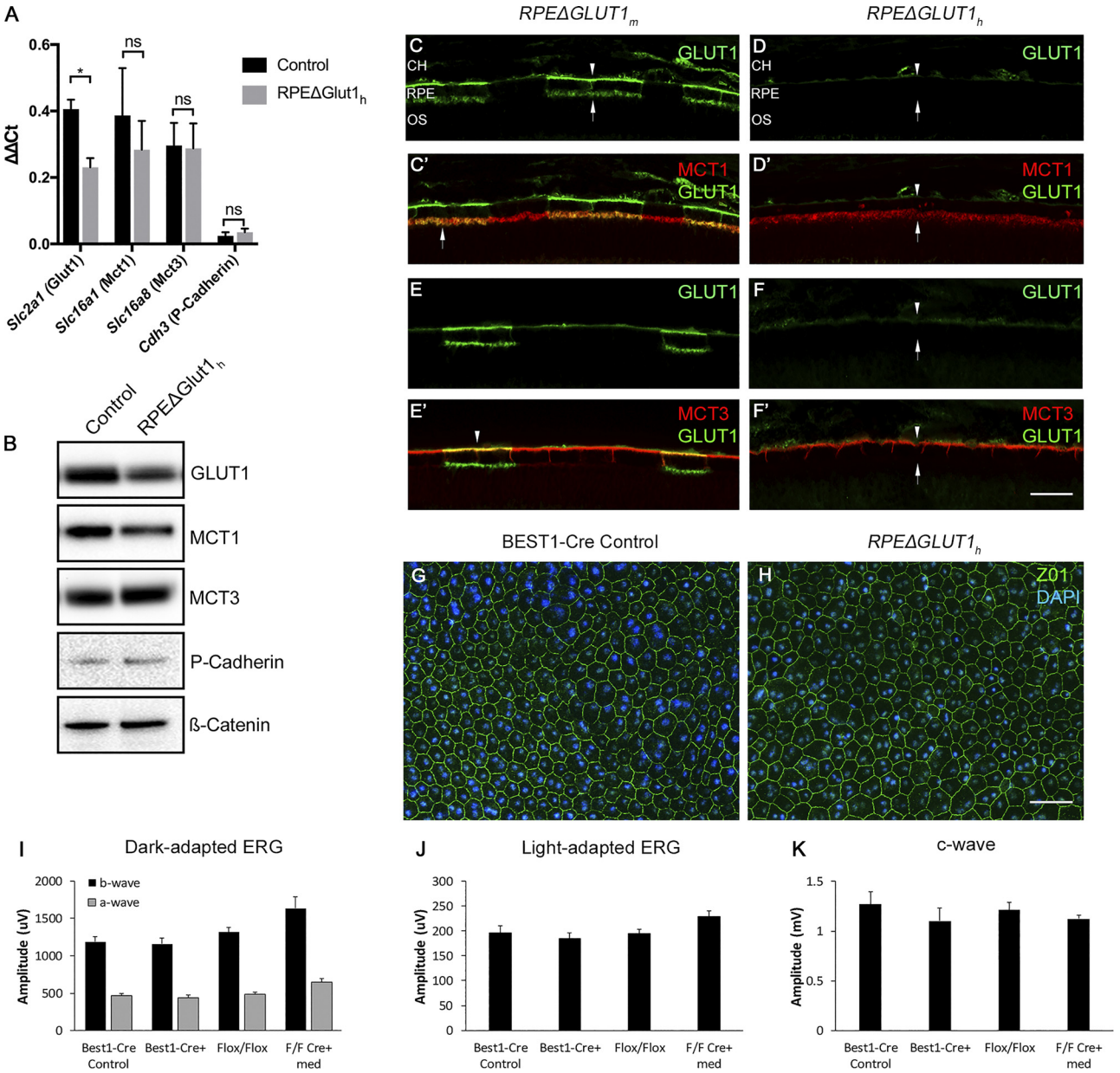

Fig. 2. Deletion of Glut1 from the RPE does not alter its polarity, differentiation, and function. *A*: quantitative PCR *of Slc2a1* (Glut1), *Slc16a1* (Mct1), *Slc16a8* (Mct3), and *Cdh3* (P-cadherin) in control ($n = 3$) and *RPEΔGlut1*$_h$ mice ($n = 3$) at 3 mo of age. *B*: Western blotting of GLUT1, MCT1, MCT3, and P-cadherin at 3 mo of age. β-Catenin was used as a loading control ($n = 3$). Immunostaining with GLUT1 (green; *C* and *D*; *E* and *F*), colabeled with MCT1 (red; *C′* and *D′*), and colabeled with MCT3 (red; *E′* and *F′*) showing that MCT1 is localized throughout the apical RPE (white arrow) and MCT3 is localized throughout the basal RPE in areas where GLUT1 is present or is deleted (white arrowheads) in areas where GLUT1 is present or is deleted in *RPEΔGlut1*$_m$ mice and *RPEΔGlut1*$_h$ mice. *G* and *H*: ZO-1 staining of RPE flatmounts shows there is no change in the hexagonal packing of RPE cells in 4-mo-old *RPEΔGlut1*$_h$ mice ($n = 3$). Scale bar, 50 μm. *I*: dark-adapted ERG averaged a- and b-wave amplitudes elicited by a 1.4 log cd·s/m^2 flash stimulus from 4- to 6-mo-old mice. *J*: light-adapted ERG average responses elicited by a 1.4 log cd·s/m^2 flash stimulus from 4- to 6-mo-old mice. *K*: c-wave averaged amplitudes from 4- to 6-mo-old mice [nontransgenic control ($n = 13$); *Best1-cre*$^+$ ($n = 9$); *Glut1*$^{flox/flox}$ ($n = 15$); *RPEΔGlut1*$_m$ mice ($n = 4$)]. *$P < 0.05$. CH, choroid; ERG, electroretinogram; MCT, monocarboxylate transporter; RPE, retinal pigment epithelium; OS, outer segments; ZO, zonula occludens.

eyes from control mice. Quantification of ONL thickness from SD-OCT scans from control and *RPEΔGlut1*$_h$ mice showed there was a 30% reduction in ONL thickness at 2 mo of age and by 50% reduction at 4 mo and 6 mo of age in *RPEΔGlut1*$_h$ mice (Fig. 4*G*). No significant changes in ONL thickness were noted in *RPEΔGlut1*$_m$ mice (Fig. 4*G*).

Glucose is essential for sustaining renewal of rod photoreceptor outer segments. Outer segment renewal is a daily process and can be slowed by inhibiting glycolysis in photoreceptor cells (5). To define the relationship between GLUT1 deletion from the RPE and outer segment shortening observed on OCT imaging and in histological sections, we compared outer segment length in retinal areas that lacked or retained GLUT1. Sections from methanol:acetic acid-fixed eyes were simultaneously probed with GLUT1 and rhodopsin antibodies. There was little change in outer segment length in *RPEΔGlut1*$_m$ retinas compared with controls (Fig. 5*A*), when GLUT1 was deleted from only a few contiguous cells (Fig.

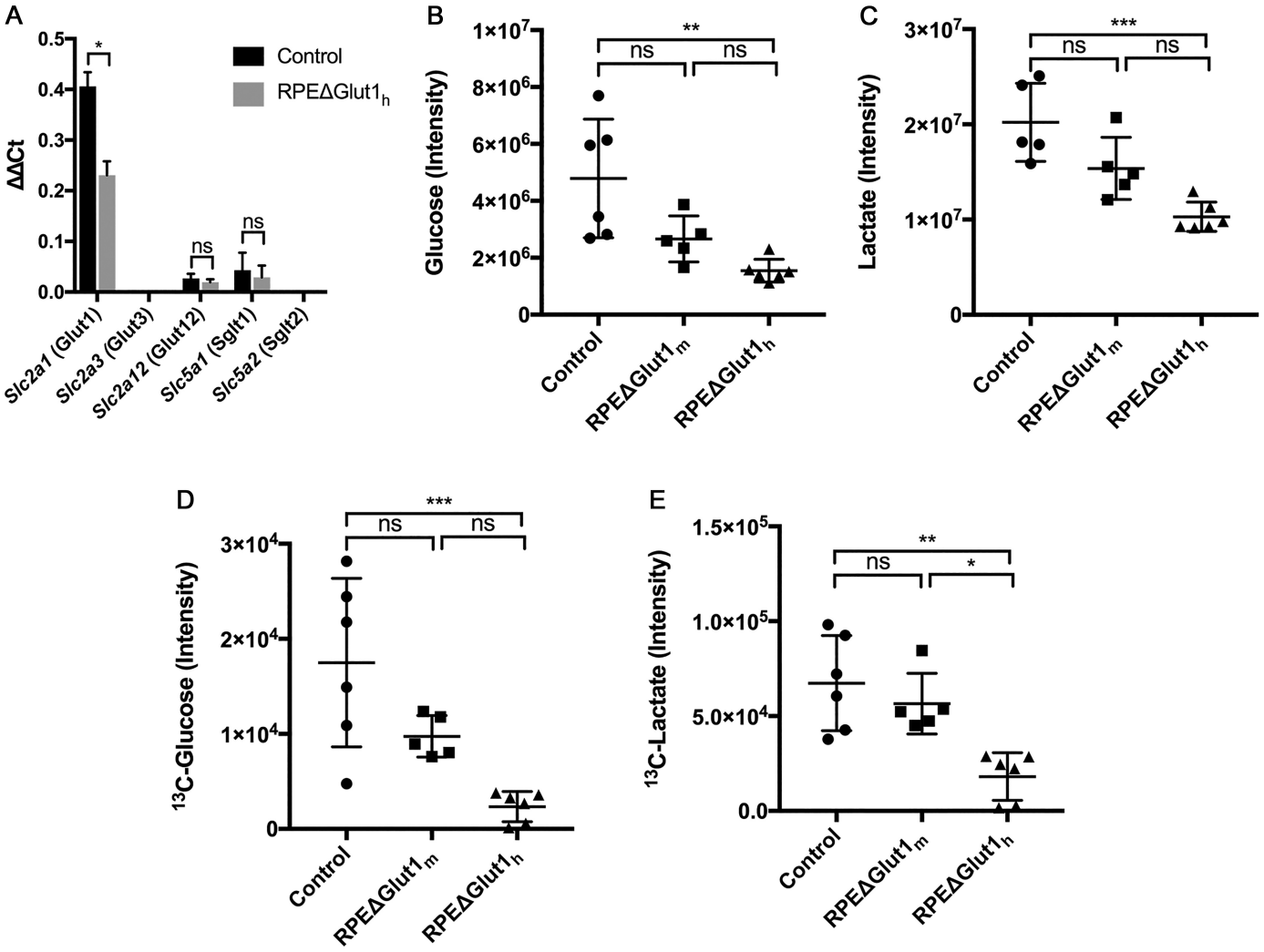

Fig. 3. *RPEΔGlut1$_h$* mice exhibit lower retinal glucose and lactate levels. *A*: quantitative PCR of glucose transporters in the RPE of 3-mo-old control ($n = 3$) and *RPEΔGlut1$_h$* mice ($n = 3$). *B*: mass spectrometry data showing that glucose is not significantly different in the retinas of *RPEΔGlut1$_m$* mice compared with controls at 4 mo ($n = 6$ from 3 mice); however, there is a 68% reduction in glucose levels in the retinas of *RPEΔGlut1$_h$* mice ($n = 6$ from 3 mice). *C*: mass spectrometry demonstrates that there is not a significant reduction in lactate levels of *RPEΔGlut1$_m$* mice while there is a 53% reduction in lactate levels in retinas of *RPEΔGlut1$_h$* mice. *D* and *E*: mass spectrometry data showing decrease in uptake of [^{13}C]glucose (*D*) and decrease in production of [^{13}C]lactate (*E*) in *RPEΔGlut1$_h$* mice compared with control and *RPEΔGlut1$_m$* mice. ANOVA was performed and $^*P < 0.05$, $^{**}P < 0.005$, $^{***}P < 0.0005$. RPE, retinal pigment epithelium.

5*B*). However, outer segments were ~30% shorter in *RPEΔGlut1$_m$* mice in areas where GLUT1 was deleted in an expanse of RPE >100 μm (Fig. 5*C*). In *RPEΔGlut1$_h$* mice, outer segments were shorter throughout the retina compared with controls (Fig. 5*D*). We next plotted outer segment length as a function of the distance from RPE cells that retained GLUT1. Representative regions measured are shown in Fig. 5*Ea*,*b*,*c*. As shown in Fig. 5*E*, outer segment shortening was detected in photoreceptor cells that were over a 100 μm from RPE expressing GLUT1. In photoreceptor cells found beyond 100 μm, there was a progressive reduction in outer segment length (Fig. 5*F*). Outer segment length was measured in retinal sections from *RPEΔGlut1$_h$* mice. Sections were colabeled with GLUT1 and rhodopsin antibodies, and outer segments were measured in the central region of the retina, 1,500 μm on either side of the optic nerve under areas where GLUT1 was deleted from the RPE. The outer segments in retinas from *RPEΔGlut1$_h$* mice were 50% shorter than outer segments in control eyes (Fig. 5*G*).

Cones are less affected by glucose deprivation than rods. To examine the impact of reduced glucose on cones, we probed retinas of 6-mo-old *RPEΔGlut1$_h$* and control mice with cone arrestin and DAPI (Fig. 6, *A* and *B*). We counted the number of cones in the central region of the retina, 1,500 μm on either side of the optic nerve. To get an accurate measurement of cone outer segment length, we also simultaneously probed the retinas with a mixture of red/green opsin and blue opsin and with GLUT1 antibodies in control (Fig. 6*C*) and 6-mo-old *RPEΔGlut1$_h$* mice (Fig. 6*D*). The number of cone arrestin-positive cells in *RPEΔGlut1$_h$* retinas was reduced by 17% as compared with controls (Fig. 6*E*). In addition, cone outer segment length was reduced by 10% in *RPEΔGlut1$_h$* retinas (Fig. 6*F*). Bearing in mind the 50% thinning of the ONL and 50% shortening of rod outer segments observed in the

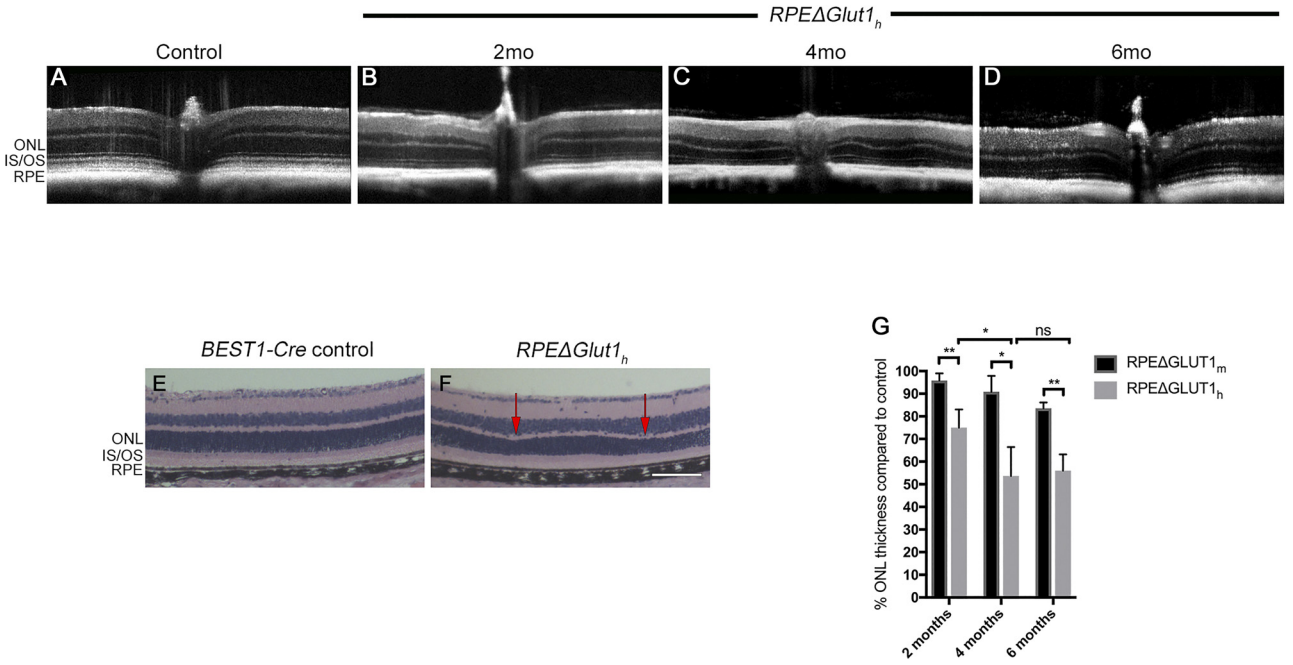

Fig. 4. Outer nuclear layer of *RPEΔGlut1$_h$* shows thinning and waviness with age. *A–D*: representative SD-OCT images of control (*A*) at 3 mo and *RPEΔGlut1$_h$* mouse imaged at 2 mo (*B*), and 4 mo (*C*) showing decrease in the ONL thickness and increase in waviness and at (*D*) 6 mo showing the stabilization of ONL thickness in *RPEΔGlut1$_h$* mice. *E* and *F*: H&E stained histological sections of 4-mo-old *Best1-Cre* control mouse (*E*) and *RPEΔGlut1$_h$* (*F*) showing waviness (represented by red arrows) in the ONL of the same animal as imaged by OCT in *A* and *B*. Scale bar, 25 μm. *G*: %ONL thickness in *RPEΔGlut1$_m$* ($n = 3$) and *RPEΔGlut1$_h$* ($n = 3$) at 2 mo, 4 mo, and 6 mo of age compared with controls. *$P < 0.05$, **$P < 0.005$. IS/OS, inner/outer segments; ONL, outer nuclear layer; RPE, retinal pigment epithelium.

RPEΔGlut1$_h$ mice at 4 mo, cones appear to be less sensitive to glucose deprivation than rods.

Glucose deprivation causes cell death in the retina and leads to upregulation of gliosis. Since we observed thinning of the ONL in *RPEΔGlut1$_h$* mice by SD-OCT, we wanted to determine whether the thinning was due to cell death occurring in the *RPEΔGlut1$_h$* mice. We performed TUNEL assay and found minimal cell death in any retinal layer of *RPEΔGlut1$_m$* mice (Fig. 7*B*). However, cell death was evident in *RPEΔGlut1$_h$* mice where it was restricted to the ONL (Fig. 7*C*). Quantification of the TUNEL assay is shown in Fig. 7*D*.

Since cell death can cause gliosis (44, 54), we wanted to determine whether glucose deprivation caused an increase in the expression of GFAP, a marker for Müller glial cell stress. In *RPEΔGlut1$_m$* mice, GFAP was not elevated when GLUT1 deletion was localized to a small patch of RPE; however, when the expanse of RPE lacking GLUT1 exceeded 35 μm, GFAP elevation was seen in the underlying retina (Fig. 7, *F, F′*, and *F′′*). The finding showed that glucose deprivation in the outer retina can cause Müller cell stress even in the absence of photoreceptor cell death. GFAP elevation occurred throughout the retina in *RPEΔGlut1$_h$* mice (Fig. 7, *G, G′, G′′*).

Amino acids support the retina under glucose deprivation conditions. The *RPEΔGlut1$_h$* retina retains ~50% of its ONL, a level which remains stable between 4 to 6 mo (Fig. 4*G*). To determine how the retina survives under conditions of glucose deprivation, we examined levels of metabolites in 3-mo-old control and *RPEΔGlut1$_h$* retinas using mass spectrometry. Significant changes are summarized in Fig. 8*A*. Levels of glutamine, glutamic acid, aspartic acid, and α-ketoglutarate were increased in *RPEΔGlut1$_h$* retina as compared with control. In contrast there was a significant decrease in intermediates of glucose metabolism through glycolysis and the pentose phosphate shunt including ribulose-5-phosphate, cGMP, and hypoxanthine (Fig. 8*A*). Next we determined whether there was an increase in expression in glutamine and glutamate transporters in the retina to compensate for the glucose deficiency in *RPEΔGlut1$_h$* retinas. There was a significant increase in levels of the amino acid transporters *Slc38a3*, *Slc1a7*, and *Slc7a8* (Fig. 8*B*). Comparing single cell microarray data of adult photoreceptor and Müller cells, we found that *Slc1a7*, which transports glutamate, was expressed at low levels by both cells types and that *Slc7a8*, which transports large neutral amino acids like glutamine and alanine, was expressed at higher levels in Müller cells compared with photoreceptors (37). *Slc38a3*, a transporter of glutamine, was expressed in both photoreceptors and Müller cells at similar levels. These findings suggest that photoreceptors survive by oxidizing other metabolic substrates such as amino acids.

DISCUSSION

Glucose is the primary metabolic substrate for neural tissue including the retina and glucose deprivation has been reported to contribute to photoreceptor loss in a number of blinding diseases (26, 50). Previous studies have demonstrated the importance of glycolysis in supporting the structure, function, and viability of photoreceptor cells by genetically deleting key glycolytic enzymes from photoreceptor cells (5, 29, 33, 34). In the current study, we disrupted glucose transport into the outer retina by genetically deleting GLUT1 from the RPE. The heterogeneity of *Best1-Cre*

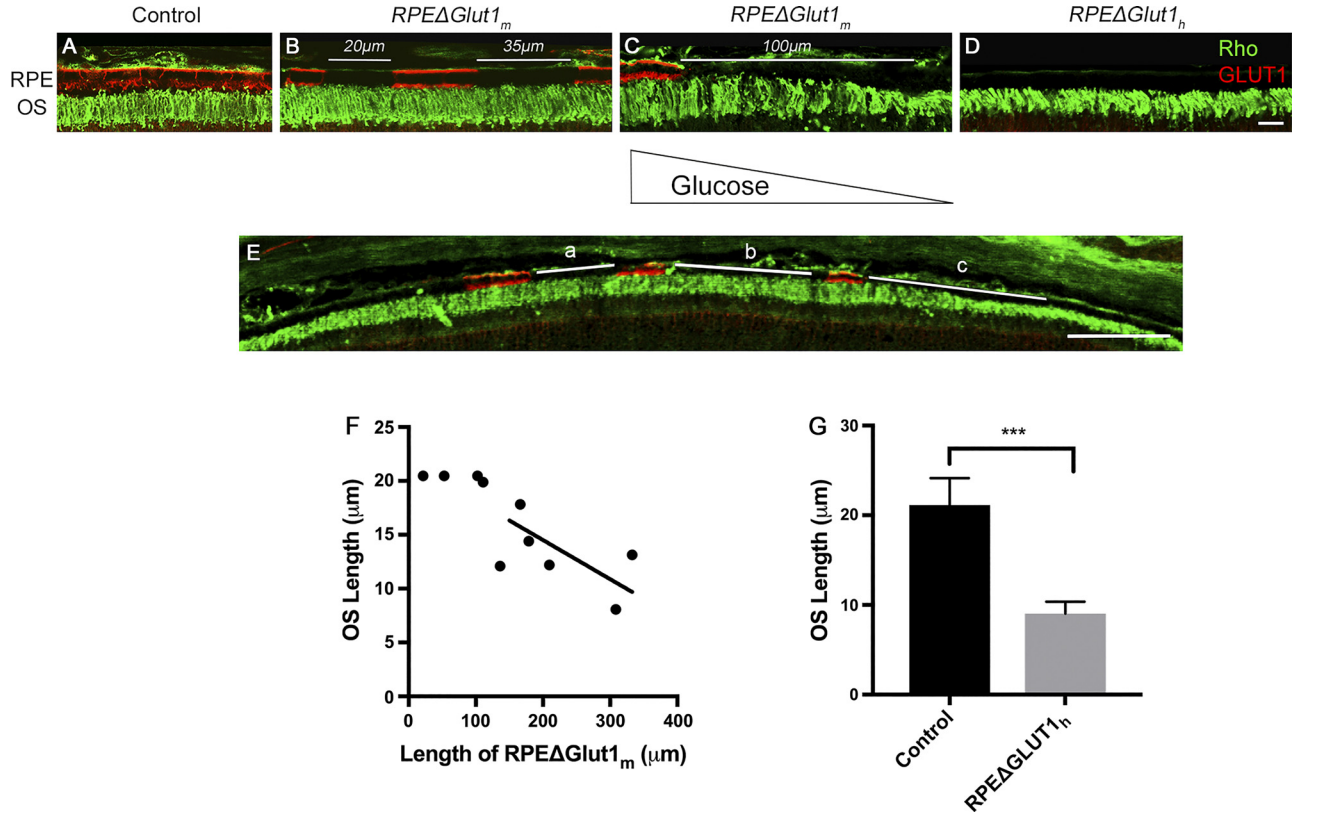

Fig. 5. Rod outer segments are shorter when GLUT1 in the RPE is deleted. *A* and *B*: methanol:acetic acid fixed sections from control (*A*) and *RPEΔGlut1*$_m$ (*B*) mice were labeled with rhodopsin (green) and GLUT1 (red) showing no difference in outer segment length when the distance of GLUT1 deletion is <100 μm. *C*: in *RPEΔGlut1*$_m$ mice with GLUT1 missing in the RPE for a distance of >100 μm there is a shortening in outer segment length ($n = 8$). *D*: *RPEΔGlut1*$_h$ mice labeled with rhodopsin and GLUT1 showing that when >70% of GLUT1 is deleted from the RPE, there is ~50% shortening of the outer segment length. Scale bar, 10 μm. *E* and *F*: ×10 image of *RPEΔGlut1*$_h$ showing the distribution of GLUT1. Representative distances were measured (*Ea*, *Eb*, *Ec*) and plotted (*F*) to show no change in OS length for regions within 100 μm of RPE cells that retain GLUT1, beyond which their outer segments become progressively shorter ($n = 4$). *G*: OS length in control vs. *RPEΔGlut1*$_h$ mice measured under where GLUT1 was deleted from the RPE ($n = 3$). All animals are 2 mo old. Scale bar, 100 μm. ***$P < 0.0005$. RPE, retinal pigment epithelium; OS, outer segments.

expression allowed us to analyze mice in which up to 50% or >70% of the GLUT1 was deleted from the RPE. In this model the flow of oxygen and other metabolites was not disrupted, providing us with a unique opportunity to better understand the importance of glucose in maintaining metabolic homeostasis in the outer retina.

An important feature of the *RPEΔGlut1* mice was that the structural and functional properties of the RPE were not altered, so the direct effects of glucose deficiency on the outer retina could be studied. Reducing the oxidative capacity of the RPE by genetically deleting *Tfam* from the RPE resulted in dedifferentiation of the RPE and secondary changes in photoreceptor cells (57). Collectively, these findings are consistent with findings from our lab and others showing that the RPE depends on oxidation of fatty acids, amino acids, and lactate, thereby sparing glucose for the outer retina (1, 9, 16, 35).

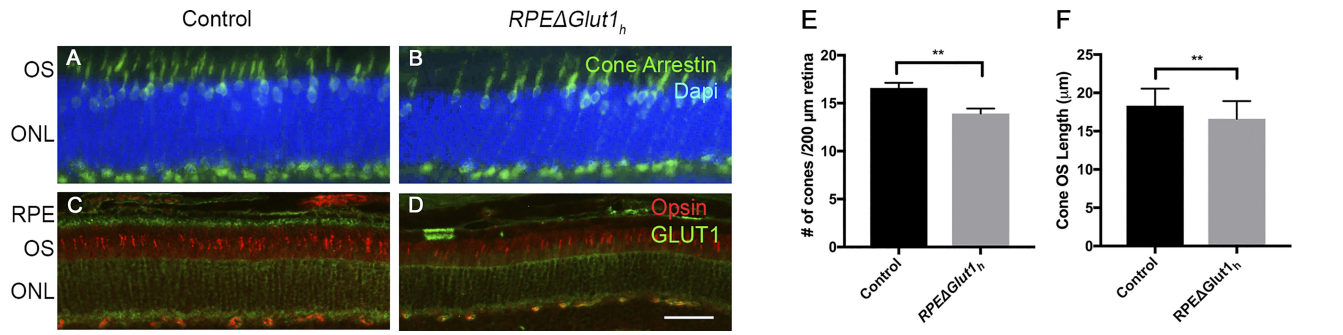

Fig. 6. Cones are less impacted than rods in *RPEΔGlut1*$_h$ mice. *A–D*: retinal sections probed with cone arrestin antibody (*A* and *B*) and red/green opsin, blue opsin antibodies and co-labeled with GLUT1 antibody (*C* and *D*) in control vs *RPEΔGlut1*$_h$ mice. *E*: quantification of cone arrestin stained cones showed 17% fewer cones in the *RPEΔGlut1*$_h$ mice compared with control in 6-mo-old mice ($n = 3$). *F*: cone outer segment length measured using red/green/blue opsin staining showing 10% reduction in cone outer segment length in *RPEΔGlut1*$_h$ mice compared with control at 6 mo ($n = 3$). **$P < 0.005$. ONL, outer nuclear layer; OS, outer segments; RPE, retinal pigment epithelium.

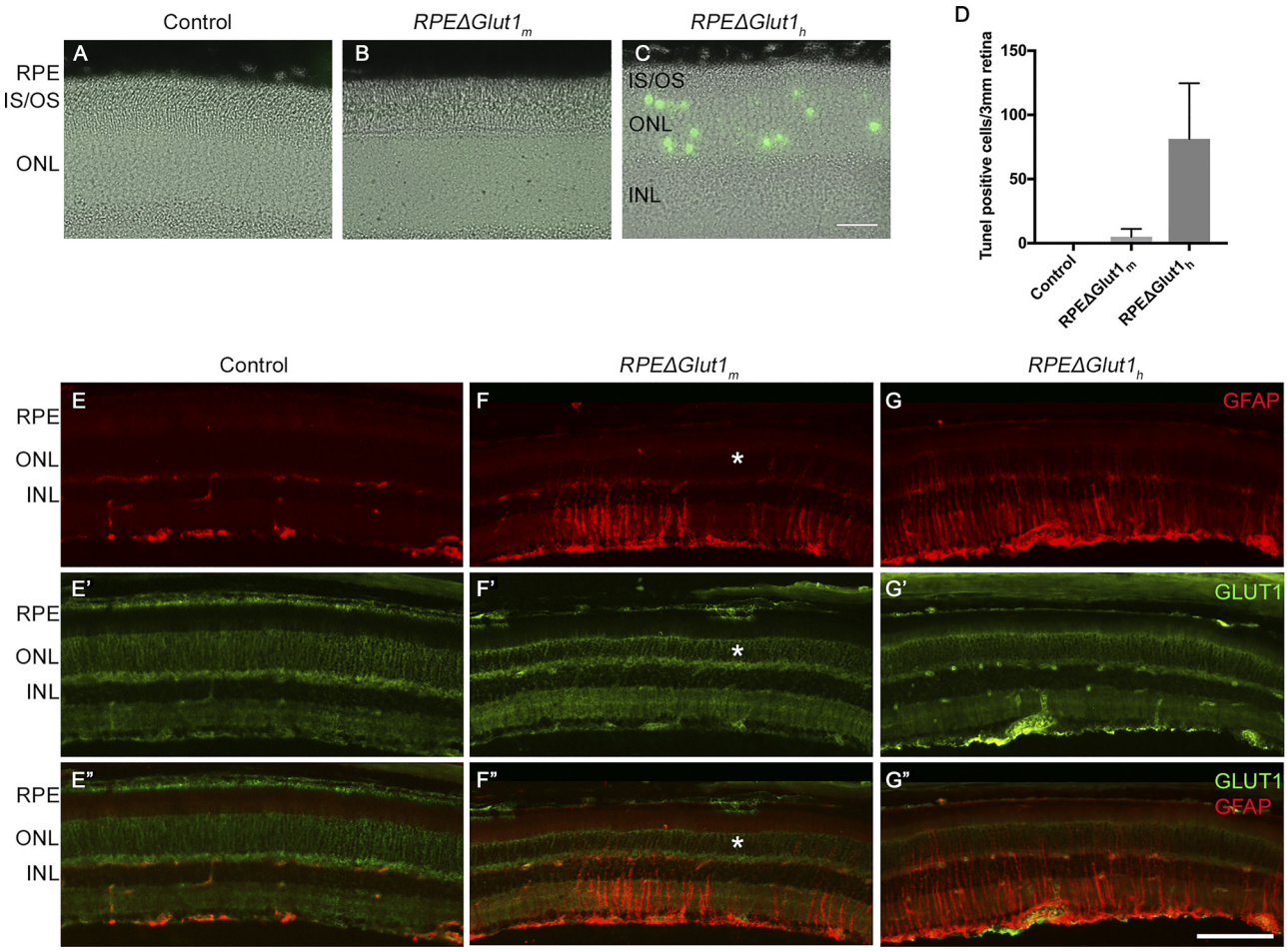

Fig. 7. Cell death and gliosis occur when GLUT1 is deleted from the RPE. The decrease in ONL thickness corresponds with cell death in the ONL as observed by TUNEL staining. *A–C*: cell death (green) was detected in *RPEΔGlut1$_h$* at 2 mo of age in control (*A*), *RPEΔGlut1$_m$* (*B*), and *RPEΔGlut1$_h$* mice (*C*). *D*: quantification of TUNEL positive cells in control ($n = 3$), *RPEΔGlut1$_m$* ($n = 3$), and *RPEΔGlut1$_h$* ($n = 3$). Scale bar, 50 μm. *E–G*: immunolabeling of control (*E*, *E′*, and *E″*), *RPEΔGlut1$_m$* mice (*F*, *F′*, and *F″*), and *RPEΔGlut1$_h$* mice (*G*, *G′*, and *G″*) with GFAP (red) and GLUT1 (green) antibodies showed upregulation of GFAP when the distance of GLUT1 deleted was >35 μm in *RPEΔGlut1$_m$* and *RPEΔGlut1$_h$* mice at 4 mo of age ($n = 6$). Asterisk indicates the region where GFAP was not upregulated in *RPEΔGlut1$_m$* mice. Scale bar, 50 μm. ONL, outer nuclear layer; IS/OS, inner/outer segments; RPE, retinal pigment epithelium.

LC/MS analysis of neural retina metabolites showed that, under steady-state conditions, glucose levels in retinas from *RPEΔGlut1$_h$* mice were 68% lower than in control retinas. In mice given a single injection of [^{13}C]glucose and retinas isolated 45 min later, LC/MS analysis showed that glucose was 87% lower in *RPEΔGlut1$_h$* than control retinas. [^{13}C]lactate was 73% lower in *RPEΔGlut1$_h$* than control retinas. The decreased level of glucose in the retina is consistent with

A

Fold Change	Sample Name	P Value
1.621	Glutamine	0.000
1.417	Aspartic Acid	0.004
1.269	Glutamic acid	0.021
1.268	α-ketoglutarate	0.033
0.769	Proline	0.031
0.718	cGMP	0.012
0.648	Ribulose 5 Phosphate	0.017
0.359	hypoxanthine	0.019

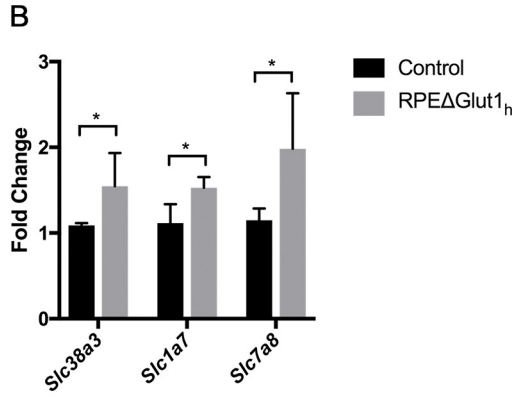

Fig. 8. Amino acid transporters are upregulated under glucose deprivation conditions. *A*: summary of amino acids and other metabolites that were upregulated (green) or downregulated (red) when glucose is reduced in the retina in 4-mo-old mice. *B*: quantitative PCR showing upregulation in different amino acid transporters ($n = 3$) in 3-mo-old mice. *$P < 0.05$.

previous studies that showed more than 60% of the blood flow to the retina is from the choroidal vessels (57). The decrease in lactate is also consistent with literature which showed 80–90% of the glucose transported into the outer retina is metabolized through aerobic glycolysis to produce lactate (51, 53). Our results clearly demonstrate that GLUT1 regulates the transepithelial flux of glucose across the RPE into the outer retina.

In *RPEΔGlut1$_m$* mice, glucose levels were similar to controls, indicating that even with only half of the cells expressing GLUT1, the transport of glucose into the outer retina could be maintained. ERGs recorded from *RPEΔGlut1$_m$* mice were comparable to those of control animals. Under dark-adapted conditions, there was a normal ERG a-wave, reflecting primarily the response of rod photoreceptors (36). Similarly, normal ERG b-waves were observed under both dark- and light-adapted conditions and reflecting primarily the activity of rod or cone depolarizing bipolar cells, respectively (18, 42). Additionally, *Glut1$^{+/-}$* heterozygote mice have ERGs that are comparable to those of wild-type littermates (40). These results mirror patients with GLUT1 deficiency who present with neurological but no visual deficits (55).

Previous studies suggested that glycolytic metabolism of glucose is required for outer segment renewal (5). Photoreceptors are distinguished from other neurons because during postnatal development there is an increase in expression of glycolytic genes including HK1, HK2, and PFKFB2 [RetSeq database (17)], while possessing large numbers of mitochondria and consuming large amounts of oxygen, both in the light and in the dark (12). It has been proposed that, like cancer cells, the photoreceptors utilize glycolysis to generate metabolic intermediates required for protein and phospholipid synthesis (5, 53). In the case of the photoreceptors, these intermediates are required for outer segment renewal. It was recently shown that transient knockdown of LDHA or PKM2, two enzymes in the glycolytic pathway, from rod photoreceptors using shRNA resulted in about a 50% shortening of outer segments (5). However, when PKM2 was genetically deleted from rod photoreceptors, there was only about a 15% reduction in outer segment length, suggesting that there was metabolic adaptation and that rods could utilize alternate pathways to generate intermediates required for disk morphogenesis (33). Similarly, we found in *RPEΔGlut1$_h$* mice, glucose deprivation resulted in shortening of outer segments throughout the retina. In *RPEΔGlut1$_m$* mice, decrease in outer segment length was only observed in photoreceptors in regions of the RPE larger than 100 μm that were not expressing GLUT1. These finding suggest that if glucose falls below a certain threshold then outer segment renewal is impaired. Although Rajala et al. (33) observed a decrease in outer segment length 5 mo after PKM2 deletion from rods, they did not observe a significant decrease in ONL thickness. In the current study, we found that, in the *RPEΔGlut1$_h$* mice, where glucose levels in the retina were reduced to 32% of control animals, the phenotype was more severe than when PKM2 or LDHA were knocked out of photoreceptor cells (5). In *RPEΔGlut1$_h$* mice, there was not only a 50% reduction in outer segment length but also a 50% thinning of the ONL, reflecting photoreceptor cell death.

In *RPEΔGlut1$_h$* mice, there was an increase in photoreceptor cell death that stabilized after about a ~50% loss of photoreceptor cells. There was a greater loss of rod versus cone photoreceptor cells, supporting previous studies showing that rods are more dependent on glycolytic metabolism than cones (28). Cone survival in the context of nutrient deprivation has been reported by Petit et al. (29), who deleted *Hk2* from cones and found that cones were less dependent than rods on aerobic glycolysis under basal conditions. Although Petit et al. (29) found that photoreceptors were not dependent on *Hk2* for survival, aerobic glycolysis was required for rod function and for cone survival under stress. Here too, we found a milder impact of glucose deprivation on cones compared with rods, with respect to both cell loss and outer segment shortening. These findings suggest that cones are not solely dependent on glycolysis since we found only a 10% reduction in cone outer segment length and 17% reduction in cone cell number in *RPEΔGlut1$_h$* mice. In comparison, when oxygen and nutrients were decreased from the outer retina by deleting *Vegfa* from the RPE, cone photoreceptors were affected within 7 days (22). Combined with our results, it appears that cones are more susceptible to cell death due to oxygen than glucose deprivation. These findings suggest that glucose may not be the primary metabolic substrate of cone photoreceptor cells.

We observed an increase in expression of GFAP in Müller glial cells in *RPEΔGlut1* mice. Interestingly, in *RPEΔGlut1$_m$*, where no photoreceptor cell death was observed, GFAP was expressed in discrete patches of Müller cells in regions of retina even where only two to three contiguous RPE cells lacked GLUT1. Since reduced glucose levels causes metabolic stress in Müller cells, it would suggest that glycolysis is important for supporting their metabolic needs as suggested by Poitry-Yamate et al. (31) and Winkler et al. (54). Additionally, there was no cell death observed in the inner nuclear layer of *RPEΔGlut1$_h$* mice, suggesting that Müller cells might be able to adapt to glucose deprivation as was also observed by Winkler et al. (54).

How is it possible for 50% of the photoreceptors to survive in *RPEΔGlut1$_h$* mice? To address this question, we used LC/MS to compare metabolite levels in control and *RPEΔGlut1* retinas and found that the loss of GLUT1 resulted in increased levels of glutamate, glutamine, and aspartate, suggesting an increase in the oxidation of amino acids in the absence of glucose. We also saw a concomitant increase in the amino acid transporters in the *RPEΔGlut1$_h$* retina. Glutamate is oxidatively deaminated to generate either NADH or NADPH, critical electron carriers for anabolic reactions including the synthesis of fatty acids used in daily disk morphogenesis. The utilization of glutamate to generate α-ketoglutarate provides tricarboxylic acid (TCA) cycle intermediates and reduces the burden of pyruvate oxidation. Aspartate also feeds into oxidative metabolism via the TCA cycle to generate oxaloacetate and possibly to serve as substrate for gluconeogenesis in an effort to maintain glucose homeostasis. Müller glial cells have been previously shown to convert excess glutamate into glutamine via glutamine synthetase which is then transported into photoreceptors via *Slc38a3* (32, 38, 49). *Slc38a3* has been shown to be localized in astrocytes in the blood-brain barrier and transports glutamine for use by neurons (4, 48). We found an upregulation in *Slc38a3* in the retinas isolated from *RPEΔGlut1$_h$*. A search of publicly available databases [RetSeq (17) and single cell microarray data from Roesch et al. (37)] showed that *Slc38a3* is expressed in both Müller cells and photoreceptors, implying that upregulation of glutamine-glutamate metabolism could be supporting photoreceptor survival.

This increase in glutamine-glutamate metabolism highlights the flexibility of the photoreceptor cells to utilize other substrates in response to glucose deprivation. It is possible that this is a general response, as it is observed in other systems. For example, Fidler et al. (10) observed a similar metabolic flexibility when they deleted GLUT1 from platelets, which subsequently increased their use of amino acids. In addition, we observed a similar compensation by amino acids when we deleted GLUT1 from mouse lens epithelium and found a decrease in amino acids in the aqueous humor of transgenic mice, indicating an increase in amino acid oxidation by the mouse lens under glucose deprivation (46). Alternatively, glucose derived from the inner retinal vasculature, perhaps along with amino acid oxidation, could be sufficient to maintain the observed degree of photoreceptor viability.

SD-OCT provides an important tool for monitoring longitudinal changes in retinal morphology (25). We used SD-OCT as a diagnostic tool to observe the retinal morphology in the *RPEΔGlut1* mice. We found slight waviness in the ONL of *RPEΔGlut1*$_m$ mice; however, their ONL thickness was not affected. The waviness was more pronounced, coupled with a decrease in ONL thickness, in *RPEΔGlut1*$_h$ mice and correlated well with the percentage of RPE cells not expressing GLUT1. We further confirmed that the waviness seen in OCT images corresponds to that seen in retinal histology, thereby validating SD-OCT as a tool to predict retinal loci lacking GLUT1 in *RPEΔGlut1*$_h$ mice. We surmise that the waviness results from the intermittent shortening of either the outer segments or the ONL, making it an early indicator of nutrient deprivation. Researchers have made similar observations in studies examining the effects of drusen on retinal structure and morphology in AMD patients (15). As drusen increased, they observed localized thinning of the ONL, shortening of outer segments and gliosis, which they interpreted to reflect locally diminished metabolic substrates reaching the retina due to the physical barrier formed by the drusen.

In conclusion, these results demonstrate that GLUT1 expression in the RPE regulates transepithelial transport of glucose into the outer retina. Glucose from the choroidal blood supply and not the inner blood vessels was required to maintain photoreceptor cell outer segment renewal and to prevent activation of Müller glial cells. We also found glucose deprivation had a greater impact on the viability of rod photoreceptors than cone photoreceptors. Together, our findings have important implications for the development of nutrient based therapies for retinal pathologies.

ACKNOWLEDGMENTS

We thank Dr. Joshua Dunaief for providing us with the *Best1-cre* transgenic mice.

GRANTS

This work was supported by the National Eye Institute (R01 EY012042 to N. J. Philp, R01 EY026525 to K. Boesze-Battaglia and N. J. Philp, and core grant P30 EY025585 to N. S. Peachey), the Department of Veterans Affairs (I01 BX002340 to N. S. Peachey and I01 BX002754 to I. S. Samuels), and Research to Prevent Blindness.

DISCLOSURES

No conflicts of interest, financial or otherwise, are declared by the authors.

AUTHOR CONTRIBUTIONS

N.S.P. and N.J.P. conceived and designed research; A.S., I.S.S., J.Y.H., and J.D. performed experiments; A.S., E.M., N.S.P., and N.J.P. analyzed data; A.S., I.S.S., B.A.B., N.S.P., and N.J.P. interpreted results of experiments; A.S. and I.S.S. prepared figures; A.S. drafted manuscript; A.S., I.S.S., J.Y.H., K.B.-B., N.S.P., and N.J.P. edited and revised manuscript; A.S., I.S.S., B.A.B., J.Y.H., J.D., E.M., E.D.A., K.B.-B., N.S.P., and N.J.P. approved final version of manuscript.

REFERENCES

1. **Adijanto J, Du J, Moffat C, Seifert EL, Hurley JB, Philp NJ.** The retinal pigment epithelium utilizes fatty acids for ketogenesis. Implications for metabolic coupling with the outer retinas. *J Biol Chem* 289: 20570–20582, 2014. doi:10.1074/jbc.M114.565457.
2. **Adijanto J, Philp NJ.** Cultured primary human fetal retinal pigment epithelium (hfRPE) as a model for evaluating RPE metabolism. *Exp Eye Res* 126: 77–84, 2014. doi:10.1016/j.exer.2014.01.015.
3. **Amram B, Cohen-Tayar Y, David A, Ashery-Padan R.** The retinal pigmented epithelium—from basic developmental biology research to translational approaches. *Int J Dev Biol* 61: 225–234, 2017. doi:10.1387/ijdb.160393ra.
4. **Chan K, Busque SM, Sailer M, Stoeger C, Bröer S, Daniel H, Rubio-Aliaga I, Wagner CA.** Loss of function mutation of the Slc38a3 glutamine transporter reveals its critical role for amino acid metabolism in the liver, brain, and kidney. *Pflügers Arch* 468: 213–227, 2016. doi:10.1007/s00424-015-1742-0.
5. **Chinchore Y, Begaj T, Wu D, Drokhlyansky E, Cepko CL.** Glycolytic reliance promotes anabolism in photoreceptors. *eLife* 6: e25946, 2017. doi:10.7554/eLife.25946.
6. **Cohen LH, Noell WK.** Glucose catabolism of rabbit retina before and after development of visual function. *J Neurochem* 5: 253–276, 1960. doi:10.1111/j.1471-4159.1960.tb13363.x.
7. **Collin GB, Hubmacher D, Charette JR, Hicks WL, Stone L, Yu M, Naggert JK, Krebs MP, Peachey NS, Apte SS, Nishina PM.** Disruption of murine Adamtsl4 results in zonular fiber detachment from the lens and in retinal pigment epithelium dedifferentiation. *Hum Mol Genet* 24: 6958–6974, 2015. doi:10.1093/hmg/ddv399.
8. **Cunha-Vaz J, Bernardes R, Lobo C.** Blood-retinal barrier. *Eur J Ophthalmol* 21, *Suppl* 6: S3–S9, 2011. doi:10.5301/EJO.2010.6049.
9. **Du J, Rountree A, Cleghorn WM, Contreras L, Lindsay KJ, Sadilek M, Gu H, Djukovic D, Raftery D, Satrústegui J, Kanow M, Chan L, Tsang SH, Sweet IR, Hurley JB.** Phototransduction influences metabolic flux and nucleotide metabolism in mouse retina. *J Biol Chem* 291: 4698–4710, 2016. doi:10.1074/jbc.M115.698985.
10. **Fidler TP, Campbell RA, Funari T, Dunne N, Balderas Angeles E, Middleton EA, Chaudhuri D, Weyrich AS, Abel ED.** Deletion of GLUT1 and GLUT3 reveals multiple roles for glucose metabolism in platelet and megakaryocyte function. *Cell Rep* 20: 881–894, 2017. doi:10.1016/j.celrep.2017.06.086.
11. **Georgiadis A, Tschernutter M, Bainbridge JWB, Balaggan KS, Mowat F, West EL, Munro PMG, Thrasher AJ, Matter K, Balda MS, Ali RR.** The tight junction associated signalling proteins ZO-1 and ZONAB regulate retinal pigment epithelium homeostasis in mice. *PLoS One* 5: e15730, 2010. doi:10.1371/journal.pone.0015730.
12. **Gospe SM III, Baker SA, Arshavsky VY.** Facilitative glucose transporter Glut1 is actively excluded from rod outer segments. *J Cell Sci* 123: 3639–3644, 2010. doi:10.1242/jcs.072389.
13. **Hirata Y, Nishiwaki H.** The choroidal circulation assessed by laser-targeted angiography. *Prog Retin Eye Res* 25: 129–147, 2006. doi:10.1016/j.preteyeres.2005.08.001.
14. **Iacovelli J, Zhao C, Wolkow N, Veldman P, Gollomp K, Ojha P, Lukinova N, King A, Feiner L, Esumi N, Zack DJ, Pierce EA, Vollrath D, Dunaief JL.** Generation of Cre transgenic mice with postnatal RPE-specific ocular expression. *Invest Ophthalmol Vis Sci* 52: 1378–1383, 2011. doi:10.1167/iovs.10-6347.
15. **Johnson PT, Lewis GP, Talaga KC, Brown MN, Kappel PJ, Fisher SK, Anderson DH, Johnson LV.** Drusen-associated degeneration in the retina. *Invest Ophthalmol Vis Sci* 44: 4481–4488, 2003. doi:10.1167/iovs.03-0436.
16. **Kanow MA, Giarmarco MM, Jankowski CS, Tsantilas K, Engel AL, Du J, Linton JD, Farnsworth CC, Sloat SR, Rountree A, Sweet IR, Lindsay KJ, Parker ED, Brockerhoff SE, Sadilek M, Chao JR, Hurley JB.** Biochemical adaptations of the retina and retinal pigment epithelium support a metabolic ecosystem in the vertebrate eye. *eLife* 6: e28899, 2017. doi:10.7554/eLife.28899.
17. **Kim J-W, Yang H-J, Brooks MJ, Zelinger L, Karakülah G, Gotoh N, Boleda A, Gieser L, Giuste F, Whitaker DT, Walton A, Villasmil R, Barb JJ, Munson PJ, Kaya KD, Chaitankar V, Cogliati T, Swaroop A.**

NRL-regulated transcriptome dynamics of developing rod photoreceptors. *Cell Rep* 17: 2460–2473, 2016. doi:10.1016/j.celrep.2016.10.074.

18. **Kofuji P, Ceelen P, Zahs KR, Surbeck LW, Lester HA, Newman EA.** Genetic inactivation of an inwardly rectifying potassium channel (Kir4.1 subunit) in mice: phenotypic impact in retina. *J Neurosci* 20: 5733–5740, 2000. doi:10.1523/JNEUROSCI.20-15-05733.2000.
19. **Kumagai AK.** Glucose transport in brain and retina: implications in the management and complications of diabetes. *Diabetes Metab Res Rev* 15: 261–273, 1999. doi:10.1002/(SICI)1520-7560(199907/08)15:4<261::AID-DMRR43>3.0.CO;2-Z.
20. **Kumagai AK, Glasgow BJ, Pardridge WM.** GLUT1 glucose transporter expression in the diabetic and nondiabetic human eye. *Invest Ophthalmol Vis Sci* 35: 2887–2894, 1994.
21. **Kurihara T, Westenskow PD, Bravo S, Aguilar E, Friedlander M.** Targeted deletion of Vegfa in adult mice induces vision loss. *J Clin Invest* 122: 4213–4217, 2012. doi:10.1172/JCI65157.
22. **Kurihara T, Westenskow PD, Gantner ML, Usui Y, Schultz A, Bravo S, Aguilar E, Wittgrove C, Friedlander MS, Paris LP, Chew E, Siuzdak G, Friedlander M.** Hypoxia-induced metabolic stress in retinal pigment epithelial cells is sufficient to induce photoreceptor degeneration. *eLife* 5: e14319, 2016. doi:10.7554/eLife.14319.
23. **Lattin JE, Schroder K, Su AI, Walker JR, Zhang J, Wiltshire T, Saijo K, Glass CK, Hume DA, Kellie S, Sweet MJ.** Expression analysis of G protein-coupled receptors in mouse macrophages. *Immunome Res* 4: 5, 2008. doi:10.1186/1745-7580-4-5.
24. **Lehmann GL, Benedicto I, Philp NJ, Rodriguez-Boulan E.** Plasma membrane protein polarity and trafficking in RPE cells: past, present and future. *Exp Eye Res* 126: 5–15, 2014. doi:10.1016/j.exer.2014.04.021.
25. **Lin P, Mettu PS, Pomerleau DL, Chiu SJ, Maldonado R, Stinnett S, Toth CA, Farsiu S, Mruthyunjaya P.** Image inversion spectral-domain optical coherence tomography optimizes choroidal thickness and detail through improved contrast. *Invest Ophthalmol Vis Sci* 53: 1874–1882, 2012. doi:10.1167/iovs.11-9290.
26. **Narayan DS, Chidlow G, Wood JPM, Casson RJ.** Glucose metabolism in mammalian photoreceptor inner and outer segments. *Clin Experiment Ophthalmol* 45: 730–741, 2017. doi:10.1111/ceo.12952.
27. **Nickla DL, Wallman J.** The multifunctional choroid. *Prog Retin Eye Res* 29: 144–168, 2010. doi:10.1016/j.preteyeres.2009.12.002.
28. **Noell WK.** The impairment of visual cell structure by iodoacetate. *J Cell Comp Physiol* 40: 25–55, 1952. doi:10.1002/jcp.1030400104.
29. **Petit L, Ma S, Cipi J, Cheng SY, Zieger M, Hay N, Punzo C.** Aerobic glycolysis is essential for normal rod function and controls secondary cone death in retinitis pigmentosa. *Cell Rep* 23: 2629–2642, 2018. doi:10.1016/j.celrep.2018.04.111.
30. **Philp NJ, Yoon H, Grollman EF.** Monocarboxylate transporter MCT1 is located in the apical membrane and MCT3 in the basal membrane of rat RPE. *Am J Physiol Regul Integr Comp Physiol* 274: R1824–R1828, 1998.
31. **Poitry-Yamate CL, Poitry S, Tsacopoulos M.** Lactate released by Müller glial cells is metabolized by photoreceptors from mammalian retina. *J Neurosci* 15: 5179–5191, 1995. doi:10.1523/JNEUROSCI.15-07-05179.1995.
32. **Poitry S, Poitry-Yamate C, Ueberfeld J, MacLeish PR, Tsacopoulos M.** Mechanisms of glutamate metabolic signaling in retinal glial (Müller) cells. *J Neurosci* 20: 1809–1821, 2000. doi:10.1523/JNEUROSCI.20-05-01809.2000.
33. **Rajala A, Wang Y, Brush RS, Tsantilas K, Jankowski CSR, Lindsay KJ, Linton JD, Hurley JB, Anderson RE, Rajala RVS.** Pyruvate kinase M2 regulates photoreceptor structure, function, and viability. *Cell Death Dis* 9: 240, 2018. doi:10.1038/s41419-018-0296-4.
34. **Rajala A, Wang Y, Soni K, Rajala RVS.** Pyruvate kinase M2 isoform deletion in cone photoreceptors results in age-related cone degeneration. *Cell Death Dis* 9: 737, 2018. doi:10.1038/s41419-018-0712-9.
35. **Reyes-Reveles J, Dhingra A, Alexander D, Bragin A, Philp NJ, Boesze-Battaglia K.** Phagocytosis-dependent ketogenesis in retinal pigment epithelium. *J Biol Chem* 292: 8038–8047, 2017. doi:10.1074/jbc.M116.770784.
36. **Robson JG, Frishman LJ.** Dissecting the dark-adapted electroretinogram. *Doc Ophthalmol* 95: 187–215, 1998. doi:10.1023/A:1001891904176.
37. **Roesch K, Jadhav AP, Trimarchi JM, Stadler MB, Roska B, Sun BB, Cepko CL.** The transcriptome of retinal Müller glial cells. *J Comp Neurol* 509: 225–238, 2008. doi:10.1002/cne.21730.
38. **Rueda EM, Johnson JE Jr, Giddabasappa A, Swaroop A, Brooks MJ, Sigel I, Chaney SY, Fox DA.** The cellular and compartmental profile of mouse retinal glycolysis, tricarboxylic acid cycle, oxidative phosphorylation, and ~P transferring kinases. *Mol Vis* 22: 847–885, 2016.
39. **Saksens NTM, Krebs MP, Schoenmaker-Koller FE, Hicks W, Yu M, Shi L, Rowe L, Collin GB, Charette JR, Letteboer SJ, Neveling K, van Moorsel TW, Abu-Ltaif S, De Baere E, Walraedt S, Banfi S, Simonelli F, Cremers FPM, Boon CJF, Roepman R, Leroy BP, Peachey NS, Hoyng CB, Nishina PM, den Hollander AI.** Mutations in CTNNA1 cause butterfly-shaped pigment dystrophy and perturbed retinal pigment epithelium integrity. *Nat Genet* 48: 144–151, 2016. doi:10.1038/ng.3474.
40. **Samuels I, Tarchick M, Trobenter TD, Kozlowski MR.** Systemic reduction of GLUT1 prevents hallmarks of diabetic retinopathy (Abstract). *Investig Ophthalmol Vis Sci* 59: 5361, 2018.
41. **Samuels IS, Sturgill GM, Grossman GH, Rayborn ME, Hollyfield JG, Peachey NS.** Light-evoked responses of the retinal pigment epithelium: changes accompanying photoreceptor loss in the mouse. *J Neurophysiol* 104: 391–402, 2010. doi:10.1152/jn.00088.2010.
42. **Sharma S, Ball SL, Peachey NS.** Pharmacological studies of the mouse cone electroretinogram. *Vis Neurosci* 22: 631–636, 2005. doi:10.1017/S0952523805225129.
43. **Steinberg RH, Linsenmeier RA, Griff ER.** Retinal pigment epithelial cell contributions to the electroretinogram and electrooculogram. *Prog Retinal Res* 4: 33–66, 1985. doi:10.1016/0278-4327(85)90004-5.
44. **Subirada PV, Paz MC, Ridano ME, Lorenc VE, Vaglienti MV, Barcelona PF, Luna JD, Sánchez MC.** A journey into the retina: Müller glia commanding survival and death. *Eur J Neurosci* 47: 1429–1443, 2018. doi:10.1111/ejn.13965.
45. **Sun N, Shibata B, Hess JF, FitzGerald PG.** An alternative means of retaining ocular structure and improving immunoreactivity for light microscopy studies. *Mol Vis* 21: 428–442, 2015.
46. **Swarup A, Bell BA, Du J, Han JYS, Soto J, Abel ED, Bravo-Nuevo A, FitzGerald PG, Peachey NS, Philp NJ.** Deletion of GLUT1 in mouse lens epithelium leads to cataract formation. *Exp Eye Res* 172: 45–53, 2018. doi:10.1016/j.exer.2018.03.021.
47. **Takata K.** Glucose transporters in the transepithelial transport of glucose. *J Electron Microsc (Tokyo)* 45: 275–284, 1996. doi:10.1093/oxfordjournals.jmicro.a023443.
48. **Todd AC, Marx M-C, Hulme SR, Bröer S, Billups B.** SNAT3-mediated glutamine transport in perisynaptic astrocytes *in situ* is regulated by intracellular sodium. *Glia* 65: 900–916, 2017. doi:10.1002/glia.23133.
49. **Umapathy NS, Li W, Mysona BA, Smith SB, Ganapathy V.** Expression and function of glutamine transporters SN1 (SNAT3) and SN2 (SNAT5) in retinal Müller cells. *Invest Ophthalmol Vis Sci* 46: 3980–3987, 2005. doi:10.1167/iovs.05-0488.
50. **Umino Y, Everhart D, Solessio E, Cusato K, Pan JC, Nguyen TH, Brown ET, Hafler R, Frio BA, Knox BE, Engbretson GA, Haeri M, Cui L, Glenn AS, Charron MJ, Barlow RB, Dowling JE.** Hypoglycemia leads to age-related loss of vision. *Proc Natl Acad Sci USA* 103: 19541–19545, 2006. doi:10.1073/pnas.0604478104.
51. **Wang L, Törnquist P, Bill A.** Glucose metabolism in pig outer retina in light and darkness. *Acta Physiol Scand* 160: 75–81, 1997. doi:10.1046/j.1365-201X.1997.00131.x.
52. **Wei H, Xun Z, Granado H, Wu A, Handa JT.** An easy, rapid method to isolate RPE cell protein from the mouse eye. *Exp Eye Res* 145: 450–455, 2016. doi:10.1016/j.exer.2015.09.015.
53. **Winkler BS.** Glycolytic and oxidative metabolism in relation to retinal function. *J Gen Physiol* 77: 667–692, 1981. doi:10.1085/jgp.77.6.667.
54. **Winkler BS, Arnold MJ, Brassell MA, Puro DG.** Energy metabolism in human retinal Müller cells. *Invest Ophthalmol Vis Sci* 41: 3183–3190, 2000.
55. **Winkler EA, Nishida Y, Sagare AP, Rege SV, Bell RD, Perlmutter D, Sengillo JD, Hillman S, Kong P, Nelson AR, Sullivan JS, Zhao Z, Meiselman HJ, Wenby RB, Soto J, Abel ED, Makshanoff J, Zuniga E, De Vivo DC, Zlokovic BV.** GLUT1 reductions exacerbate Alzheimer's disease vasculo-neuronal dysfunction and degeneration. *Nat Neurosci* 18: 521–530, 2015. doi:10.1038/nn.3966.
56. **Yang X, Chung J-Y, Rai U, Esumi N.** Cadherins in the retinal pigment epithelium (RPE) revisited: P-cadherin is the highly dominant cadherin expressed in human and mouse RPE in vivo. *PLoS One* 13: e0191279, 2018. doi:10.1371/journal.pone.0191279.
57. **Zhao C, Yasumura D, Li X, Matthes M, Lloyd M, Nielsen G, Ahern K, Snyder M, Bok D, Dunaief JL, LaVail MM, Vollrath D.** mTOR-mediated dedifferentiation of the retinal pigment epithelium initiates photoreceptor degeneration in mice. *J Clin Invest* 121: 369–383, 2011. doi:10.1172/JCI44303.
58. **Zhu S, Yam M, Wang Y, Linton JD, Grenell A, Hurley JB, Du J.** Impact of euthanasia, dissection and postmortem delay on metabolic profile in mouse retina and RPE/choroid. *Exp Eye Res* 174: 113–120, 2018. doi:10.1016/j.exer.2018.05.032.